Freezing of liquid alkali metals as screened ionic plasmas

1991 J. Phys.: Condens. Matter 3 1627

(http://iopscience.iop.org/0953-8984/3/11/020)

J. Phys.: Condens. Matter 3 (1991) 1627–1636. Printed in the UK

Freezing of liquid alkali metals as screened ionic plasmas

Z Badirkhan†, M Rovere‡ and M P Tosi‡§

† International School for Advanced Studies, Trieste, Italy
‡ Department of Theoretical Physics, University of Trieste, Trieste, Italy
§ International Centre for Theoretical Physics, Trieste, Italy

Received 1 August 1990, in final form 26 November 1990

Abstract. The relationship between Wigner crystallization of the classical ionic plasma and the liquid–solid transition of alkali metals is examined within the density wave theory of freezing. Freezing of the classical plasma on a rigid neutralizing background into the BCC structure is first re-evaluated, in view of recent progress in the determination of its thermodynamic functions by simulation and of the known difficulties of the theory relating to the order parameter at the (200) star of reciprocal lattice vectors. Freezing into the FCC structure is also considered in this context and found to be not favoured. On allowing for long-wavelength deformability of the background, the ensuing appearance of a volume change on freezing into the BCC structure is accompanied by reduced stability of the fluid phase and by an increase in the entropy of melting. Freezing of alkali metals into the BCC structure is next evaluated, taking their ionic pair structure as that of an ionic plasma reference fluid screened by conduction electrons and requiring that the correct ionic coupling strength at liquid–solid coexistence should be approximately reproduced. The ensuing values of the volume and entropy changes across the phase transition, as estimated from the theory by two alternative routes, are in reasonable agreement with experiment. The order parameters of the phase transition, excepting the (200) one, conform rather closely to Gaussian behaviour and yield a Lindemann ratio in reasonable agreement with the empirical value for melting of BCC crystals. It is suggested that ionic order at the (200) star in the metal may be assisted by medium-range ordering in the conduction electrons, as indicated by differences in X-ray and neutron diffraction intensities from the liquid, and/or quite small in the hot BCC solid. Such a possible premelting behaviour of BCC metals should be worth testing experimentally by diffraction.

1. Introduction

The classical one-component plasma (OCP) of point charges on a uniform neutralizing background has been considered by many workers as a reference fluid for perturbative calculations of thermodynamic and structural properties of liquid metals (Minoo *et al* 1977, Khanna and Cyrot-Lackmann 1979, Ross *et al* 1981, Mon *et al* 1981, Chaturvedi *et al* 1981a, Young 1982, Itami and Shimoji 1984, Iwamatsu *et al* 1984, Montella *et al* 1984, Pastore and Tosi 1984, Ono and Yokohama 1984, 1987, 1989, Iwamatsu 1985, Khanna and Shanker 1985a, b, 1986, Bratkovsky 1988, Lai 1988). This choice of reference system is particularly successful for the liquid alkali metals and the main conclusions of direct present interest that have emerged for these metals from the above

0953-8984/91/111627 + 10 $03.50

theoretical work may be summarized as follows. The OCP structure factor at the appropriate value of the coupling strength parameter $\Gamma = e^2/ak_BT$, where T is the temperature of the liquid metal and $a = (4\pi n/3)^{-1/3}$ in terms of the atomic number density n, reproduces surprisingly well the measured structure factor of real alkali metals near freezing, except in the small-angle scattering region. A significantly lower value is obtained for the plasma parameter appropriate to the liquid metal when it is determined variationally from the Gibbs–Bogoliubov inequality for the Helmholtz free energy, leading to some deterioration in the predicted structure factor and to improved agreement with the measured values of the excess entropy in the liquid. Finally, an optimized perturbative treatment of the electron-screening interactions shows that the modifications induced by electronic screening in the ionic structure factor are indeed crucial at long wavelengths but are essentially confined to wavenumbers well below the main peak.

There are also some empirical similarities between the liquid–solid transition of the alkali metals and the freezing of the OCP. The alkalis freeze at standard pressure into BCC crystals at temperatures T_m such that the values of the ion–ion coupling strength e^2/ak_BT_m are in the range from 210 for Li and Na to 180 for Cs, whereas crystallization of the OCP occurs into the BCC structure at $\Gamma = 178$ (Brush *et al* 1966, Pollock and Hansen 1973, Slattery *et al* 1980, 1982, Ogata and Ichimaru 1987, DeWitt *et al* 1990) and into the FCC structure at $\Gamma = 192$ (Helfer *et al* 1984, DeWitt *et al* 1990), the latter structure being clearly metastable. The entropy change on melting of the alkalis is in the range $\Delta S_m/k_B = 0.80$–0.85 and thus close to that of the OCP ($\Delta S_m = 0.78k_B$ for the BCC crystal). On the other hand, a distinctly small, but finite, volume change on melting ($\Delta v_m/v = 0.016$ for Li and 0.025–0.026 for the other alkalis) reflects the finite compressibility of the metal, whereas the OCP model is commonly taken to have no volume change on melting. Measurements of the melting curve of Na under pressure by Ivanov *et al* (1973) indicate that the ionic coupling strength at melting tends to a value of about 150 as the volume change on melting tends to zero with increasing pressure.

The combination of the forementioned theoretical results for the ionic pair structure of the liquid alkalis and of empirical facts relating to their liquid–solid transition suggests that a primitive view of the phase transition could be obtained by regarding the liquid phase near freezing as a classical ionic plasma embedded on a background which is endowed with deformability at long wavelengths to allow for perfect screening of the ions by the conduction electrons and for a finite compressibility of the system. Indeed, within the framework of the density wave theory of freezing (Ramakrishnan and Yussouff 1977, 1979), the phase transition is associated with the spontaneous appearance of order parameters which are driven, at the simplest level of approximation, by the liquid compressibility and by the structure factor at wavenumbers corresponding to the various stars of reciprocal lattice vectors (RLVs) of the crystal. The first star of RLVs, i.e. the (110) star for the BCC lattice, approximately corresponds to the main peak in the liquid structure factor and thus lies in a wavenumber region such that electronic screening is already essentially immaterial in determining the ionic pair structure of the liquid metal.

The above picture of the liquid–solid transition in alkali metals, although appealing because of its simplicity, needs careful examination. The predictions of the density wave approach for freezing of the OCP on a rigid background (OCP-RB) have been examined by a number of workers (Haymet 1984, Rovere and Tosi 1985, Barrat 1987, Barrat *et al* 1988, Iyetomi and Ichimaru 1988). These calculations have given evidence for an important role of higher-order correlations in the fluid phase in assisting the phase transition. In essence, the fluid structure of the OCP, while appropriately soft to modulation in the (110) star of the RLVs of the BCC lattice, is rigid against modulation in the

(200) star, which must therefore be assisted by couplings to other order parameters. Extrapolating these considerations to freezing of alkali metals, one expects that special attention should be given to the volume change and to the (110) and (200) sets of microscopic order parameters. An earlier evaluation of the phase transition in Na (Ramakrishnan and Yussouff 1979) has included only the (110) and (211) microscopic order parameters, corresponding to the first two peaks of the liquid structure factor.

The relative behaviour of the liquid metal and of the OCP model at the (200) star is particularly worthy of attention in view of the analysis given by Dobson (1978) (see also the review by Tamaki (1987)) of x-ray and neutron diffraction intensity data for liquid Na and Al, following an earlier proposal by Egelstaff *et al* (1974). Dobson's analysis gave evidence for some medium-range ordering of the conduction electrons in these liquid metals, which is revealed by excess x-ray scattering intensity peaking at the appropriate (111) and (200) stars. Such ordering is, of course, completely missing in the OCP model and may assist the phase transition in the liquid metal.

A discussion of the relationship between the liquid–solid transition of alkali metals and the freezing of the OCP is the object of the present paper. Its layout is briefly as follows. Section 2 collects for convenience the essential equations that are needed in our calculations. The freezing of the OCP-RB is first re-evaluated in section 3, with a view to assessing to some quantitative extent the consequences of omission of non-linear couplings between microscopic order parameters and considering also the question of the relative stability of the BCC and the FCC structure. The same section then presents similar calculations for an OCP with a deformable background (OCP-DB), to which we attribute the property of perfect screening and a mechanical stiffness chosen to reproduce the liquid compressibility of the alkalis. Finally, section 4 gives a summary of our main results and some concluding remarks.

2. Theory

We summarily present in this section the main equations that we shall use in the calculations to be reported in the following section, with specific attention to the liquid–solid transition in an OCP-DB.

The ionic density profile of the crystalline phase is

$$\rho(\boldsymbol{r}) = \rho_l \left(1 + \eta + \sum_{\boldsymbol{G}\neq 0} \rho_{\boldsymbol{G}} \exp(\mathrm{i}\boldsymbol{G}\cdot\boldsymbol{r})\right) \tag{2.1}$$

where ρ_l is the density of the fluid phase, $\rho_{\boldsymbol{G}}$ are the microscopic order parameters associated with the reciprocal lattice vectors $\boldsymbol{G}$, and $\eta = (\rho_s - \rho_l)/\rho_l = \Delta v/v_s$ gives the percentage volume difference between the two phases. Here and in the following, we use the subscripts s and l to denote macroscopic properties of the solid and fluid phase, respectively, and the symbol Δ to denote differences between fluid and solid.

Density functional theory gives the form of the Helmholtz free energy as

$$F[\rho(\boldsymbol{r})] = k_B T \int \mathrm{d}\boldsymbol{r}\, \rho(\boldsymbol{r})\{\ln[\lambda^3\rho(\boldsymbol{r})] - 1\} + \int \mathrm{d}\boldsymbol{r}\, \rho(\boldsymbol{r}) U(\boldsymbol{r}) + F_e[\rho(\boldsymbol{r})] \tag{2.2}$$

where λ is the thermal de Broglie wavelength, $F_e[\rho(\boldsymbol{r})]$ is the excess free-energy functional and $U(\boldsymbol{r})$ is a periodic external potential, whose microscopic Fourier components vanish at phase coexistence. The conventional density wave approach to freezing

expands the excess free energy of the solid in equation (2.2) around the fluid phase. Following Haymet and Oxtoby (1981) and D'Aguanno *et al* (1987), and including only second-order terms in the difference $\rho(r) - \rho_l$, the equilibrium condition for the microscopic order parameters can be written as

$$\rho_G = (1+\eta)\int \mathrm{d}r \exp(\mathrm{i}G\cdot r)\exp\Big(c_0\eta + \sum_{G\neq 0} c_G\rho_G \exp(\mathrm{i}G\cdot r)\Big)\Big/\int \mathrm{d}r \exp\Big(c_0\eta + \sum_{G\neq 0} c_G\rho_G \exp(\mathrm{i}G\cdot r)\Big). \tag{2.3}$$

One also obtains expressions for the difference in chemical potential, i.e.

$$\Delta\mu = k_B T \ln\Big[\frac{1}{(1+\eta)V}\int \mathrm{d}r \exp\Big(c_0\eta + \sum_{G\neq 0} c_G\rho_G \exp(\mathrm{i}G\cdot r)\Big)\Big] \tag{2.4}$$

and the difference in pressure, i.e.

$$\Delta P = \rho_l k_B T\Big(-\eta + c_0\eta + \tfrac{1}{2}c_0\eta^2 + \tfrac{1}{2}\sum_{G\neq 0} c_G|\rho_G|^2\Big). \tag{2.5}$$

In these equations, c_G are the Fourier components of the Ornstein–Zernike direct correlation function $c(r)$ of the fluid at the RLV stars of the solid:

$$c_G = \rho_l \int \mathrm{d}r\, c(r)\exp(\mathrm{i}G\cdot r) = 1 - \frac{1}{S(G)} \tag{2.6}$$

$S(k)$ being the liquid structure factor, and c_0 is the regular part of the Fourier transform of $c(r)$ at long wavelengths, which in the OCP model embodies also thermodynamic properties to be assigned to the neutralizing background. In our realization of an OCP-DB, we assume exact cancellation of the divergent Coulomb term at long wavelengths through perfect screening of the ions by the charges in the background. The conditions for phase coexistence then are

$$\Delta\mu = 0 \tag{2.7}$$

$$\Delta P = 0. \tag{2.8}$$

The quantity c_0 will be related to the isothermal compressibility K_T of the full system of ions plus background, according to the Ornstein–Zernike relation

$$c_0 = 1 - 1/S(0) = 1 - 1/\rho_l k_B T K_T. \tag{2.9}$$

We remark before proceeding that, in the case of an OCP-RB (freezing at constant density), the equations derived by previous workers (see, e.g., Rovere and Tosi 1985) follow at once from equations (2.3)–(2.5) by setting $\eta = 0$. In this case, however, the coexistence condition is given by the vanishing of the Helmholtz free-energy difference, i.e.

$$\Delta F/N = \Delta\mu - \Delta P/\rho_l = 0 \tag{2.10}$$

yielding from equations (2.4) and (2.5), after self-consistent solution of equations (2.3), the value Γ_c of the plasma parameter at phase coexistence. Equation (2.4) (with $\eta = 0$) then allows an estimate of the interfacial dipole layer between the two phases. Furthermore, the entropy ΔS_m of melting per particle is unambiguously obtained as

$$\Delta S_m = -k_B T[\partial(\Delta F/N)/\partial T]_V = k_B \Gamma \, d(\Delta F/Nk_B T)/d\Gamma \tag{2.11}$$

evaluated at $\Gamma = \Gamma_c$.

Let us return to equations (2.3)–(2.9). As discussed in detail by D'Aguanno *et al* (1987), this set of equations can be solved by two alternative routes, in relation to the determination of the macroscopic parameters of the phase transition. One may impose first the condition (2.7) and obtain from equation (2.4) an equation for η:

$$1 + \eta = \frac{1}{V}\int d\boldsymbol{r} \exp\left(c_0\eta + \sum_{G\neq 0} c_G \rho_G \exp(i\boldsymbol{G}\cdot\boldsymbol{r})\right) \tag{2.12}$$

to be solved self-consistently together with equations (2.3) for ρ_G. Coexistence is determined in this case by the condition (2.8) and ΔS_m can be obtained from the slope of ΔP in equation (2.5) at coexistence, using the basic thermodynamic relation

$$\Delta S_m = [k_B T/(1+\eta)][\partial(\Delta P/\rho_l k_B T)/\partial T]_\mu + [\eta/(1+\eta)]S_l. \tag{2.13}$$

S_l in equation (2.13) is the entropy per particle of the fluid phase at freezing. Alternatively, one may impose first the condition (2.8) to obtain η and ρ_G from equations (2.3) and (2.5) and subsequently use equation (2.7) to determine coexistence. In this case, one obtains from the slopes of $\Delta\mu$ at coexistence.

$$\Delta S_m = -[\partial(\Delta\mu)/\partial T]_P \tag{2.14}$$

$$\eta/(1+\eta) = \rho_l^2 K_T[\partial(\Delta\mu)/\partial\rho_l]_T. \tag{2.15}$$

Of course, these alternative routes to the thermodynamic quantities ΔS_m (from equation (2.13) or equation (2.14)) and $\eta_m = \Delta v_m/v_s$ (from equations (2.12), (2.8) or (2.15)) should yield identical results in an exact theory. We shall show below the numerical magnitude of the inconsistencies that arise from using an approximate theory.

Finally, in order to emphasize the relationship between the microscopic order parameters ρ_G and the Debye–Waller factors of the crystal at melting we write

$$\rho_G = (1+\eta)\exp(-\tfrac{1}{6}L_G^2 G^2 d^2) \tag{2.16}$$

where $d = (3\pi^2)^{1/6}a$ is the first-neighbour distance in the BCC lattice and L_G is a star-dependent 'Lindemann ratio', which would become independent of G in the harmonic approximation for the Bragg scattering intensities from the crystal. The variance of these quantities with G tests the accuracy of a Gaussian representation for the single-particle density in the crystal at melting, while their magnitude is directly related to Lindemann's empirical criterion for melting of BCC crystals.

3. Results

The common input to all the calculations to be reported in this section is the direct correlation function $c(k)$ of the OCP as a function of the plasma parameter Γ. We evaluate this function by the generalized mean spherical approximation (GMSA) of Chaturvedi *et al* (1981b), using as input the new expression for the internal energy of the OCP as a function of Γ given by DeWitt *et al* (1990). Only very small differences are found in $c(k)$ relative to earlier refined calculations in the relevant range of values of Γ. Our results at $\Gamma = 160$ are reported for later reference in figure 1, in superposition with the locations of the stars of RLVs for both the BCC and the FCC lattice. Show in the same figure are also

the results of earlier GMSA calculations (Rovere and Tosi 1985); the slight differences in the region of the main minimum of $c(k)$ represent an improvement in the already excellent agreement with the available simulation data.

Using this input we first solve the set of equations (2.3) for the microscopic order parameters ρ_G as functions of Γ in the case of freezing of the OCP-RB into the BCC lattice, monitoring at the same time the free-energy difference in equation (2.10). The method of solution is the same as that of Rovere and Tosi (1985). We again find no self-consistent solution of equations (2.3) and (2.10) when the order parameter $\rho_{(200)}$ at the (200) star is included among the others to be determined from the appropriate equation (2.3), but excluding the latter we obtain satisfactory convergence in the results by including the stars of RLVs up to the (433) star, in groups which lie between alternate nodes of $c(k)$. Our results for the phase transition show only small numerical differences from theirs, owing to the small differences in input, and are reported as a starting point for further discussion in the first row of table 1. These results refer to the arbitrary choice $\rho_{(200)} = 0$, as indicated just above, and the corresponding predicted value for Γ_c (=157) is somewhat too low. This choice is approximately equivalent for the OCP-RB to an estimate of three-body correlations (Iyetomi and Ichimaru 1988) and, in parallel with their work, we find that a very modest allowance for order at the (200) star ($\rho_{(200)} \simeq 0.004$) or a drastic increase in the corresponding value of $c_{(200)}$ (from -0.50 to -0.13) is needed to reproduce the value of Γ_c (=178) from computer simulation data. The predicted value of ΔS_m correspondingly decreases to $0.94k_B$ from the value of $1.0k_B$ reported in the table, thus reducing the discrepancy with the simulation data ($\Delta S_m = 0.78k_B$). The last part of the first row in table 1 reports the predicted values of the Lindemann ratio at the (110), (211) and (220) stars, as well as the average $\langle L \rangle$ of the Lindemann ratios for the stars from (310) to (433), the average deviation from their mean value being also shown. Clearly, the single-particle density in the OCP crystal at melting, except its Fourier component at the (200) star, conforms rather closely to a Gaussian. The magnitude of our Lindemann ratios for the OCP-RB is in good agreement with the simulation data of Pollock and Hansen (1973) on the mean square displacement of the ions from their lattice sites as a function of Γ.

Before proceeding to illustrate the consequences of deformability of the background on the above phase transition, we pause to discuss briefly, as far as our approximate theoretical approach allows, the question of the relative stability of the FCC and BCC structures for the OCP-RB. Reference to the locations of the stars of RLVs for these two structures relative to the peaks and valleys of $c(k)$ in figure 1 indicates that they may be competitive, insofar as in both the first RLV star is close to the maximum in the main peak of $c(k)$ and a number of order parameters lie in the region of the subsequent deep minimum of this function. The relative stability of the two structures should thus be primarily determined by a balance between the higher number of order parameters lying in this region for the FCC structure and the more strongly negative value attained by $c_{(200)}$ for freezing into the BCC structure. In the microscopic calculations that we have carried out for freezing into the FCC lattice, we have been able to obtain a self-consistent solution of equations (2.3) and (2.10) only by excluding the order parameter at the (220) star and in this case we find that $\Gamma_c \simeq 300$. These results are broadly consistent with the available evidence from computer simulation (DeWitt *et al* 1990) in suggesting that freezing into the FCC structure is not favoured and confirm an earlier report by Barrat and Hansen (1989).

Let us now turn to present our calculations for freezing of an OCP-DB into the BCC lattice and their relation to freezing of the alkali metals. The first issue here is the value

Table 1. Parameters of freezing into the BCC lattice for the OCP-RB and for an OCP-DB corresponding to $S(0) = 0.023$. The data in the row labelled Alkalis refer to alkali metals at atmospheric pressure.

	Γ_c	$\rho_{(200)}/(1+\eta_m)$	$c_{(200)}$	$\Delta S_m/k_B$	η_m	$L_{(110)}$	$L_{(200)}$	$L_{(211)}$	$L_{(220)}$	$\langle L \rangle$
OCP-RB	157	0	−0.50	1.0	0	0.171	∞	0.159	0.155	0.146 ± 0.003
OCP-DB	146	0	−0.48	1.39[a], 1.18[b]	0.063[c], 0.009[d]	0.162	∞	0.152	0.149	0.141 ± 0.002
	202	0.01	−0.61	1.31[a], 1.10[b]	0.087[c], 0.008[d]	0.141	0.487	0.135	0.132	0.124 ± 0.002
	202	0.48	−0.35	1.04[a], 0.86[b]	0.050[c], 0.007[d]	0.194	0.194	0.175	0.162	0.156 ± 0.006
Alkalis	180–210	—	−0.6	0.80–0.85	0.016–0.026	Lindemann ratio at melting ≃ 0.12[e], 0.15[f]				

[a] From equation (2.13), with $\eta_m S_l = 0.19 k_B$ as appropriate to liquid Na.
[b] From equation (2.14).
[c] From equation (2.12); the values of η_m following from equation (2.8) are essentially the same.
[d] From equation (2.15).
[e] Calculated in the Debye approximation by Faber (1972).
[f] Calculated in the harmonic approximation by Chaturvedi *et al* (1981a).

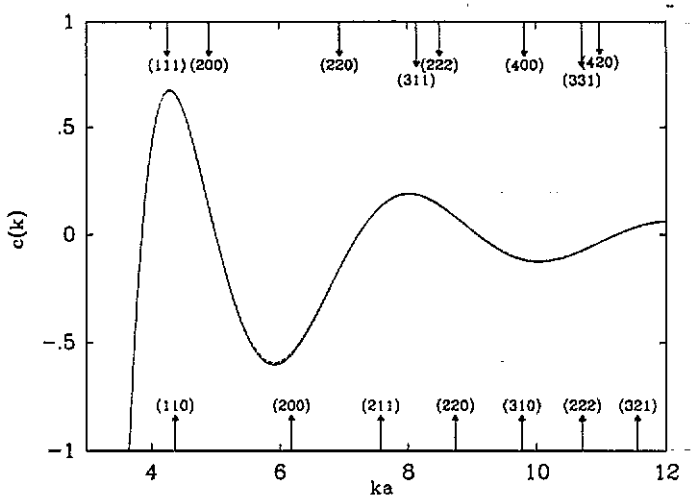

Figure 1. The Ornstein–Zernike direct correlation function $c(k)$ of the OCP at $\Gamma = 160$ as a function of reduced wavenumber ka: ——, present GMSA results, using the internal energy of the OCP from DeWitt *et al* (1990); – – –, GMSA results from the earlier internal energy data of Slattery *et al* (1980). The arrows give the locations of the stars of RLVs for the BCC lattice (bottom) and for the FCC lattice (top).

to be chosen for the quantity c_0 expressing this deformability, or equivalently for the long-wavelength structure factor $S(0) = (1 - c_0)^{-1}$. The values of $S(0)$ which are available in the literature for liquid alkali metals near freezing (Webber and Stephens 1968, Greenfield *et al* 1971, Huijben and van der Lugt 1979, Waseda 1980) are typically in the range 0.021–0.026. We have carried out calculations for a few values of $S(0)$ over this range, finding results that are not significantly different except for the value of the relative volume change η_m. Naturally, this value increases with increasing $S(0)$. We have accordingly chosen to report only the results that we obtain for the typical choice $S(0) = 0.023$. This quantity is kept fixed during our search for the coexistence point, so that the latter is simply specified by the appropriate coupling strength Γ_c for the underlying ionic plasma which describes the microscopic ionic pair structure of the liquid metal.

The results for freezing of the OCP-DB in the second row of table 1 have been obtained under the assumption that $\rho_{(200)} = 0$ and are thus directly comparable with those for the OCP-RB in the first row. The main qualitative changes which accompany the appearance of a finite volume change across the phase transition are

(a) a decrease in the value of Γ_c, i.e. reduced stability of the fluid phase as first pointed out by Pollock and Hansen (1973),

(b) an increase in the entropy of melting and

(c) a narrowing of the single-particle distribution around each lattice site in the hot solid.

We also notice that there is a reasonable amount of internal thermodynamic consistency in the calculation of ΔS_m and in the calculation of η_m from the conditions (2.7) and (2.8), whereas the route leading to a value of η_m via equation (2.15) yields a very different result.

Among the consequences of background deformability that we have seen above, (b) is in qualitative agreement with the data on the entropy of melting of alkali metals relative to that of the OCP-RB, while (a) is in disagreement with the evidence that we have quoted in section 1 for melting of alkali metals both at atmospheric pressure ($\Gamma_c = 180$–210 against $\Gamma_c = 178$ for the OCP-RB) and under pressure (Γ_c decreasing with decreasing volume change across the phase transition). The most likely source of uncertainty in our results is, of course, the handling of ordering at the (200) star. Two alternative extreme viewpoints could be taken with regard to this failure of the theory. These are

(i) the (200) order parameter is genuinely small in the hot BCC crystal or

(ii) microscopic couplings between the ionic order parameters and (in the case of alkali metals) between these and electronic order parameters assist ordering in the (200) star.

Clearly, our approach does not allow us to discriminate between these possibilities, which may in fact be simultaneously correct. We examine their separate consequences immediately below.

In the third and fourth rows of table 1 we report the results that we obtain when we ask which value of $\rho_{(200)}$, or alternatively of $c_{(200)}$, would be compatible with a value of Γ_c for the OCP-DB lying in the range appropriate for alkali metals at standard pressure. These may be compared both with our earlier results in the second row and with empirical data for alkali metals in the last row. The viewpoint (ii) gives overall better agreement with the data and it is remarkable that in this case the Lindemann ratio at the (200) star near melting falls in the general pattern set by the others. However, in view also of the fact that the diffraction patterns from the liquid alkalis show that the separation between first and second neighbours in the BCC solid has been obliterated on melting, we feel that the viewpoint (i) cannot be completely rejected. We also stress that microscopic couplings imply an effective change in $c_{(200)}$ which is more than one order of magnitude larger than the error in the liquid metal structure coming from our omission of electronic screening (see the values of $c_{(200)}$ in the last three rows of table 1).

4. Concluding remarks

We have examined in this work a simple model for the liquid–solid transition of the alkali metals, which is suggested by an interpretation of their ionic pair structure in the liquid as that of a classical ionic plasma with long-wavelength screening by the conduction electrons. We have seen that this simple picture yields, within the quantitative uncertainties that affect the theory of the phase transition, a reasonable account of its thermodynamic parameters and of the state of order obtaining in the BCC solid at melting.

We have focused attention in our discussion on the behaviour of the Fourier transform of the periodic crystalline density at the (200) star of RLVs. The difficulties of the theory in this connection are qualitatively similar to those already well known for Wigner crystallization of the classical plasma on a rigid background. Our results suggest that the phase transition in the alkali metals may also be assisted by medium-range ordering of the conduction electrons in the liquid, which is indicated by differences of x-ray and neutron scattering intensities from liquid Na as analysed by Dobson (1978). However, it is also possible that anharmonicity in hot BCC crystals may appear as a premelting phenomenon through a rapid decrease in scattering intensity at the (200) Bragg diffraction spots.

Acknowledgment

We acknowledge sponsorship of this work by the Ministero dell'Università e della Ricerca Scientifica e Tecnologica of Italy.

References

Barrat J L 1987 *Europhys. Lett.* **3** 523
Barrat J L and Hansen J P 1989 *Simple Molecular Systems at Very High Density* ed A Polian, P Loubeyre and N Boccara (New York: Plenum) p 491
Barrat J L, Hansen J P and Pastore G 1988 *Mol. Phys.* **63** 747
Bratkovsky A M 1988 *Z. Phys. Chem.* **156** 431
Brush S G, Sahlin H L and Teller E 1966 *J. Chem. Phys.* **45** 2102
Chaturvedi D K, Rovere M, Senatore G and Tosi M P 1981a *Physica* B **111** 11
Chaturvedi D K, Senatore G and Tosi M P 1981b *Nuovo Cimento* B **62** 375
D'Aguanno B, Rovere M and Senatore G 1987 *Phys. Chem. Liquids* **16** 157
DeWitt H E, Slattery W L and Stringfellow G S 1990 *Strongly Coupled Plasma Physics* ed S Ichimaru (Amsterdam: Elsevier) p 635
Dobson P J 1978 *J. Phys. C: Solid State Phys.* **11** L295
Egelstaff P A, March N H and McGill N C 1974 *Can. J. Phys.* **52** 1651
Faber T E 1972 *Introduction to the Theory of Liquid Metals* (Cambridge: Cambridge University Press) p 104
Greenfield A J, Wellendorf J and Wiser N 1971 *Phys. Rev.* A **4** 1607
Haymet A D J 1984 *Phys. Rev. Lett.* **52** 1013
Haymet A D J and Oxtoby D W 1981 *J. Chem. Phys.* **74** 2559
Helfer H L, McCrory R L and Van Horn H M 1984 *J. Stat. Phys.* **37** 577
Huijben M J and van der Lugt W 1979 *Acta Crystallogr.* A **35** 431
Itami T and Shimoji M 1984 *J. Phys. F: Met. Phys.* **14** L15
Ivanov V A, Makarenko I N, Nikolaenko A M and Stishov S M 1973 *Phys. Lett.* **45A** 18
Iwamatsu M 1985 *Physica* B **138** 310
Iwamatsu M, Moore R A and Wang S 1984 *Phys. Lett.* **101A** 97
Iyetomi H and Ichimaru S 1988 *Phys. Rev.* B **38** 6761
Khanna S N and Cyrot-Lackmann F 1979 *J. Physique Lett.* **40** L45
Khanna K N and Shanker G 1985a *Physica* B **133** 176
—— 1985b *Phys. Chem. Liquids* **15** 69
—— 1986 *Phys. Status Solidi* b **137** K107
Lai S K 1988 *Phys. Rev.* A **38** 5707
Minoo H, Deutsch C and Hansen J P 1977 *J. Physique Lett.* **38** L191
Mon K K, Gann G and Stroud D 1981 *Phys. Rev.* A **24** 2145
Montella N, Senatore G and Tosi M P 1984 *Physica* B **124** 22
Ogata S and Ichimaru S 1987 *Phys. Rev.* A **36** 5451
Ono S and Yokoyama I 1984 *J. Phys. F: Met. Phys.* **14** 2909
—— 1987 *J. Phys. F: Met. Phys.* **17** L141
—— 1989 *Physica* B **154** 309
Pastore G and Tosi M P 1984 *Physica* B **124** 383
Pollock E L and Hansen J P 1973 *Phys. Rev.* A **8** 3110
Ramakrishnan T V and Yussouff M 1977 *Solid State Commun.* **21** 389
—— 1979 *Phys. Rev.* B **19** 2775
Ross M, DeWitt H E and Hubbard W B 1981 *Phys. Rev.* A **24** 1016
Rovere M and Tosi M P 1985 *J. Phys. C: Solid State Phys.* **18** 3445
Slattery W L, Doolen G D and DeWitt H E 1980 *Phys. Rev.* A **21** 2087
—— 1982 *Phys. Rev.* A **26** 2255
Tamaki S 1987 *Can. J. Phys.* **65** 286
Waseda Y 1980 *The Structure of Non-Crystalline Materials* (New York: McGraw-Hill) p 252
Webber G M B and Stephens R W B 1968 *Physical Acoustics* vol 4B, ed W P Mason (New York: Academic) p 53
Young W H 1982 *J. Phys. F: Met. Phys.* **12** L19